Available online at www.sciencedirect.com
SCIENCE DIRECT
Cement and Concrete Research 36 (2006) 971–978
Cement and Concrete Research

The effect of various slaked limes on the microstructure of a lime–cement–sand mortar

Y. Sébaïbi [a], R.M. Dheilly [a], B. Beaudoin [b], M. Quéneudec [a,*]

[a] Laboratoire de Technologies Innovantes, Université de Picardie Jules-Verne, I.U.T Département Génie Civil, Avenue des Facultés, 80025 Amiens Cedex 01, France
[b] Laboratoire de Réactivité et de Chimie des Solides, Université de Picardie Jules Verne, Faculté des Sciences Fondamentales et Appliquées, 33 rue Saint Leu, 80039 Amiens Cedex, France

Received 4 November 2005; accepted 18 December 2005

Abstract

The present work aims to provide a better understanding of the effect of both the proportions and the characteristics of slaked lime on the microstructure of a lime–cement–sand mortar. Cement (CPA CEM I 52.5) has been replaced by various categories of slaked lime chosen for the diversity of their physico-chemical characteristics.

Cement has been replaced by lime in proportions varying between 0 to 10% of the total binder mass. With very few exceptions, mortars were produced by maintaining the quantity of water constant.

Experimental results show that it is necessary to have a high lime substitution percentage to influence the microstructure of the mortar, except in the case of a lime containing magnesium hydroxide or calcic lime featuring sizeable specific surface area.

The influence of the nature of the substituted lime on the development of the microstructure in the matrix has been examined by SEM observations of the mortar micro porosity.
© 2006 Elsevier Ltd. All rights reserved.

Keywords: Slaked lime; Physico-chemical characteristics; Elastic modulus; Microstructure; SEM

1. Introduction

Over the past twenty years, many studies have been conducted on improving the physical and mechanical characteristics of mortars by means of adding or substituting mineral fines [1–9]. The underlying purpose of these efforts has been the protection of the environment and the conservation of energy resources, while improving mortar performance.

Even though the relationships between the microstructure and the physical properties of these new mortars have been widely discussed in these studies, it should still be noted that slaked lime has not been used often as a mineral fine.

Until now, very few scientific papers have dealt with mortars made from a mixture of slaked lime and Portland cement. Nevertheless, the research conducted by Sriboonlue and Wallo [10] merits special attention. Their work focused on the influence of the various components of a lime–cement mortar on both the mortar's mechanical strength and elastic modulus. Within the scope of their study, lime mix proportions were varied during mortar production. Philippi et al. [11] concentrated their study on the lime mortar microstructure with the aim of developing methods to analyse the microstructure of porous materials displaying a wide range of pore sizes. Upon completion of this work, Philippi proposed a three-dimensional model to represent the heterogeneous pore structure of the mortar and went on to study both water retention and humidity transfer using this model [12]. In 1996, Colantuono et al. [13] examined the capillarity phenomenon occurring in porous materials bound by lime–cement mortars. However in none of these studies was the influence of lime on the physical and chemical properties of a lime–cement mortar actually investigated.

Lime–cement mortars have started inciting renewed interest thanks to the prospect of a sizeable market for maintaining and restoring historical buildings. In light of this new development, the study of the influence of the physico-chemical characteristics

* Corresponding author. Tel./fax: +33 3 22 53 40 16.
E-mail address: michele.tkint@iut.u-picardie.fr (M. Quéneudec).

0008-8846/$ - see front matter © 2006 Elsevier Ltd. All rights reserved.
doi:10.1016/j.cemconres.2005.12.021

of lime on the evolution of lime–cement–sand mortar microstructure has been undertaken.

To target these objectives, the present work has primarily focused on a Portland cement mortar in which a portion of the cement has been replaced by lime. Mortars were produced according to one of two processes: either holding the quantity of water constant or holding the level of workability constant. In order to better determine the impact of replacing cement by lime on the development of species normally present in mortars, the chemical nature of the substituted lime has also varied.

2. Experimental

2.1. Raw materials

2.1.1. Slaked limes (Ci)

The slaked limes used in this work are those which were studied by Sébaïbi Y. et al. [14]. The main characteristics of the various limes are outlined below, and presented in Table 1.

The calcium and magnesium hydroxides used herein are pure hydroxides (i.e. of analysis-grade quality); their purities are greater than 98% and 95%, respectively. On a scanning electron micrograph, both $Ca(OH)_2$ and $Mg(OH)_2$ appear as a cluster of fine platelets measuring up to 10 μm in the case of calcium hydroxide, yet whose entanglement makes it impossible to define the exact shape [15].

The industrial limes studied herein (C_1, C_2 and C_3) are slaked limes chosen for the diversity of their physico-chemical characteristics.

Table 1
Physico-chemical characteristics of the various limes tested

Samples	$Ca(OH)_2$	$Mg(OH)_2$	C_1	C_2	C_3	C_4 [a]
CaO (total)	74.2	0.1	73.5	73.9	42.3	42.1
MgO	0.7	68.2	0.4	0.6	29.8	31.5
Fe_2O_3	0.06	<0.01	0.1	0.3	0.1	0.03
SiO_2	0.10	0.08	0.8	0.3	0.4	0.09
Al_2O_3	0.08	<0.01	0.1	0.1	0.1	0.05
SO_3	<0.01	<0.01	0.02	0.03	0.04	<0.01
$LI_{1000\ °C}$	24.8	31.1	24.4	24.3	26.7	25.63
$Ca(OH)_2$ (%)	97.4 [b]		94.4[b]	96[b]	55.2[b]	55
$Mg(OH)_2$ (%)		98.5[b]				45
S.S.(BET) (m^2/g)	15.5	6.6	17.5	41.2	28.8	11.4
Grading distribution						
1 μm	10	11	9	5	12	10
5 μm	52	37	44	38	58	52
10 μm	69	48	68	52	69	66
20 μm	82	60	85	65	78	77
32 μm	90	71	91	74	84	85
45 μm	95	89	94	80	88	93
63 μm	99.5	99.4	96	85	92	99
90 μm	99.9	100	98	90	95	100
160 μm	100	100	99.9	95	99.5	100
250 μm	100	100	100	98	100	100
500 μm	100	100	100	99	100	100

[a] The sample C_4 is a laboratory-made mix containing pure "analysis-grade" calcium and magnesium hydroxides in the same proportions as those of a hydrated dolomite.

[b] Value obtained by thermogravimetric analysis and calculated from DTA/TG curves.

Table 2
Chemical analysis and Bogue composition of the CPA CEM I cement used in mortar production

CaO	MgO	SiO_2	Fe_2O_3	Al_2O_3	SO_3	$LI_{1000\ °C}$	C_3S	C_2S	C_3A	C_4AF
64.8	0.8	21.3	4.3	3.7	2.7	1.2	62.0	14.0	2.5	13.1

Limes C_1 and C_2 have been hydrated under atmospheric pressure; their composition and purity are close to those of the pure calcium hydroxide. In the case of C_2, the tablets exhibit smaller size [15]. The specific surface area of C_1 (17.5 m^2/g) is close to that of calcium hydroxide (15.5 m^2/g), while it is not the case for lime C_2. The specific surface area of this lime (41.2 m^2/g) is 2.65 times higher than that of $Ca(OH)_2$. Lime C_3 has been hydrated under pressurised conditions [16]. This category of lime is a hydrated dolomite that differs from normally hydrated lime by: the presence of a small proportion of non-hydrated oxides (<8%), high plasticity, and a high water-retention capacity (which may be attributed to the small size of the crystals (<1 μm)).

Although lime C_2 is constituted of larger size crystals, this lime exhibits a specific surface area greater than those of the other limes. This phenomenon can be related to its more important porous volume [14].

Lime C_4 is a laboratory-made mixture containing the aforementioned pure "analysis-grade" magnesium and calcium hydroxides. These components were mixed in the same proportions as those of a hydrated dolomite (55% $Ca(OH)_2$ and 45% $Mg(OH)_2$).

Limes C_3 and C_4, whose chemical compositions are similar, appear on the scanning electron analysis as a cluster of fine particles composed of both $Ca(OH)_2$ and $Mg(OH)_2$. In the case of industrial lime C_3, which has been hydrated under pressure, this cluster appears to be more compact. Even if qualitative analyses were performed, it would be difficult to differentiate the platelets of calcium hydroxide from those of magnesium hydroxide. The specific surface area of lime C_3 is 2.5 times higher than that of C_4 [15].

2.1.2. Cement (Ce)

The cement used is CPA CEM I 52.5 (NF P 15-301). This cement was already used for previous works [14]. Its B.E.T specific surface area is 1.66 m^2/g. Its composition is presented in Table 2. This cement is a sulphate resistant cement. According to some authors this kind of cement can lead to a greater depth of carbonation [17], which could be attractive in the case of a lime–cement binder.

Table 3
W/*B* ratios as a function of substituted lime when mortars are made by holding workability constant

Ci/Ci+Ce (%)	Substituted lime					
	$Ca(OH)_2$	$Mg(OH)_2$	C_1	C_2	C_3	C_4
0	0.500	0.500	0.500	0.500	0.500	0.500
2	0.500	0.500	0.510	0.500	0.525	0.500
5	0.530	0.525	0.550	0.525	0.575	0.525
10	0.575	0.575	0.575	0.600	0.630	0.575

Ci is the mass of lime and Ce is the cement's mass.

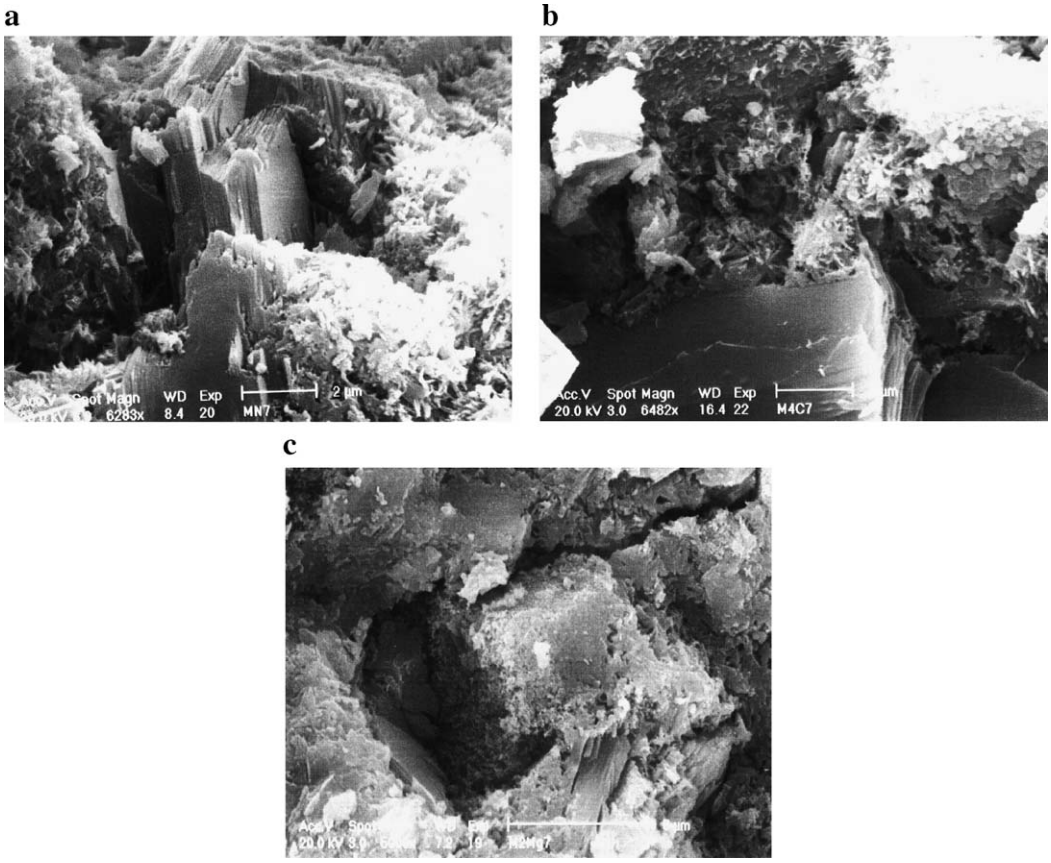

Fig. 1. Scanning electron micrographs of 7 day-old mortars, with the ratio W/B held constant, a: cement–sand reference mortar, the trace corresponds to 2 μm, b: mortar in which 4% of the cement has been replaced by $Ca(OH)_2$, the trace corresponds to 2 μm, c: mortar in which 2% of the cement has been replaced by $Mg(OH)_2$, the trace corresponds to 5 μm.

2.1.3. Sand (S)

The sand used is a siliceous sand commonly encountered as a building material in the northern French region of Picardy. It is often used in masonry coatings. XRD analysis displays the presence of a few non-siliceous components, while SEM analysis reveals the angular shape of the grains [14].

2.2. Experimental set-up

This work has focused for the most part on the microstructure of the hardened material. A scanning electron microscopy analysis of the arrangement of the various species present in the paste has been conducted to determine the impact of replacing a percentage of the cement by lime has shown the evolution of mortar microstructure.

2.2.1. Mortar production

The mortars used herein were prepared in accordance with the mass proportions for sand and binder B (Ce+Ci) stipulated in Standard EN 196-1 regarding "normal" mortars ($S/B=3$). For the mortars which were made by holding the W/B constant, this ratio was equal to 0.5. For the mortars which were produced by holding workability constant, the mix details are presented in Table 3. Mixing of the various components was performed in a standardised mortar mixer (in accordance with EN 196-1). This mixer features an orbital movement and operates at two speeds (62.5±5 and 125±10 revs/min).

2.2.2. Determination of the dynamic elastic modulus

This was undertaken by means of a supersonic auscultation method that relies on determining the propagation speed C_L of supersonic waves through the material [18].

The material is submitted to longitudinal oscillations with the help of a range of electro-acoustical transducers.

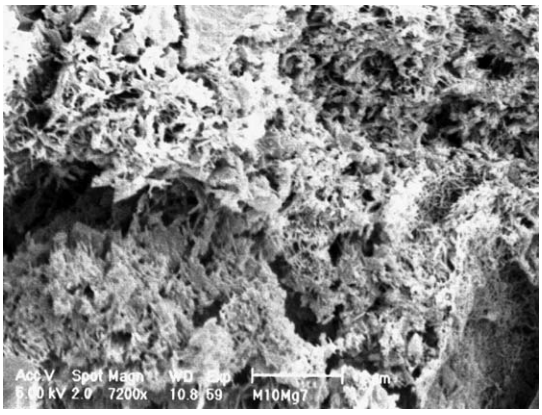

Fig. 2. Scanning electron micrograph of a 7 day-old mortar in which 10% of the cement has been replaced by $Mg(OH)_2$, with the W/B ratio held constant, the trace corresponds to 2 μm.

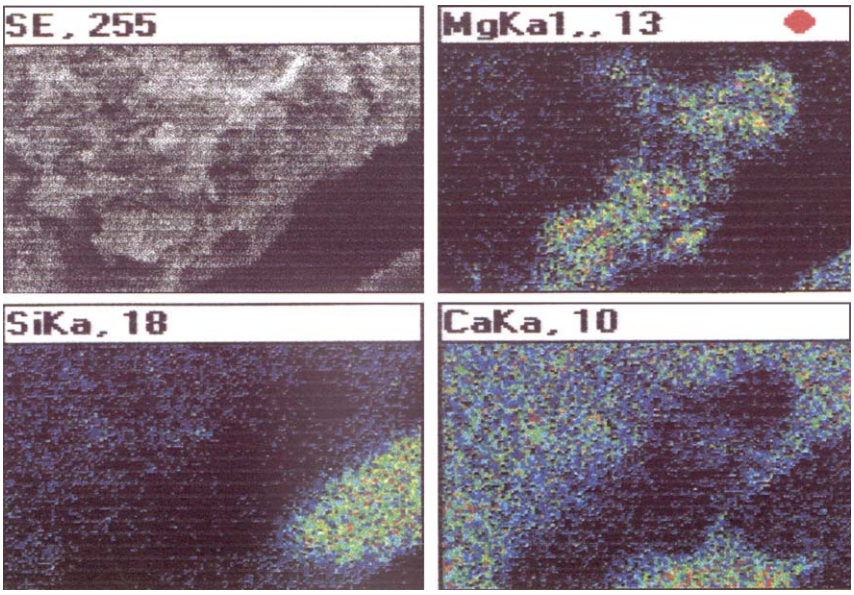

Fig. 3. Qualitative analysis of a 7 day-old mortar in which 10% of the cement has been replaced by $Mg(OH)_2$, with the W/B ratio held constant.

The dynamic elastic modulus may be deduced as follows:

$$E_d = \frac{(1+v)(1-2v)}{(1-v)} \cdot \rho \cdot C_L^2 \quad (1)$$

where C_L is wave speed (m/s); E_d is dynamic elastic modulus (N/m^2); ρ is apparent density (kg/m^3); and v is Poisson's ratio.

The equipment used in the present work consisted of a programmable dynamic numerical sounder equipped with a data storage device (a Posso Ultrasonic Tester, which complies with the NF P 18-418, NF P 18-556 and P2 EN 132-96 Standards).

The value of Poisson's ratio is dependent upon the category of concrete and generally lies between 0.2 and 0.3. Since the actual value has not been determined herein, it is assumed constant for purposes of an initial approximation, despite the changing nature of the binder. Moreover the overvalued dynamic elastic modulus has been determined

$$E_d^* = \rho \cdot C_L^2 \quad (2)$$

by setting the ratio $(1+v)(1-2v)/(1-v)$ 1.

2.2.3. Morphological analyses

Scanning electron microscopy was used to assess the morphology of materials used in these tests and then to identify the different phases present in the mortar. This analysis has, in particular, made it possible to visualise the arrangement of the various species present in the mortar paste.

The free water in the samples was removed by means of vacuum drying, and the samples were then covered with a thin layer of gold. The micrographs were generated with a PHILIPS FEG XL 30, which allows Energy Depressive X-ray (EDX) analysis during the observation period. EDX analysis allows the determination of the atomic composition of the sample.

The raw materials have also been characterised by laser granulometry. Measurements were performed by a type 850 CILAS diffraction laser; this device enables analysis over the 0.1–600 μm range.

A MICROMETRICS ASAP 2010 (with nitrogen) was used for surface area and porosity measurements. The surface area of the samples was determined by means of the BET method [19]. BET calculations provide the sample surface area value by determining the mono-layer volume of adsorbed gas from the isotherm data. The BJH (Barret–Joyner–

Table 4
Quantitative analysis of the species appearing on sides of cracks within the matrix of a 7 day-old mortar in which 10% of the cement has been replaced by magnesium hydroxide

Species	Element (%)	Atomic (%)
Mg	41.51	86.52
Si	2.68	4.84
Ca	4.38	5.54
Au	12.04	3.10
Total	60.61	100.00

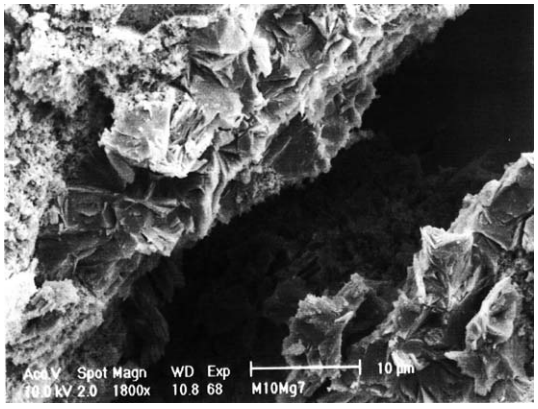

Fig. 4. Scanning electron micrograph of a 7 day-old mortar in which 10% of the cement has been replaced by magnesium hydroxide, with the W/B ratio held constant, the trace on the micrograph corresponds to 10 μm.

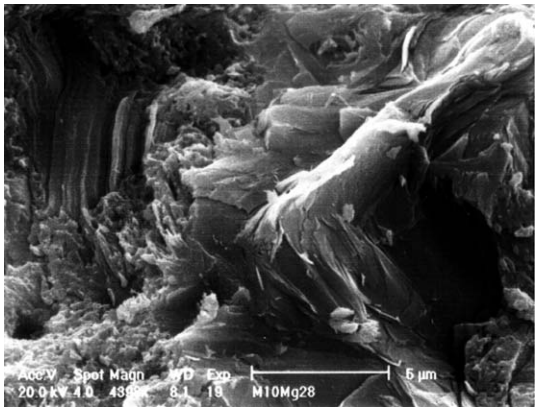

Fig. 5. Scanning electron micrograph of a 28 day-old mortar in which 10% of the cement has been replaced by magnesium hydroxide (constant W/B ratio), the trace on the micrograph corresponds to 5 µm.

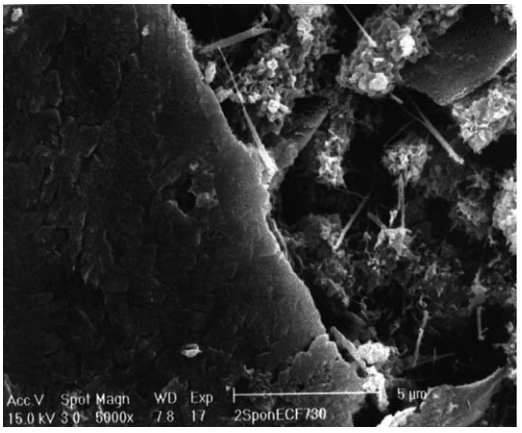

Fig. 7. Scanning electron micrograph of a mortar in which 2% of lime C_2 has been substituted, the trace on the micrograph corresponds to 5 µm.

Halenda) method was employed to obtain additional information on the pore distribution and volume of the various samples [20]. This measurement also allows the determination of the pore volume and mass density of pores whose radii are in the range of r and $r+\mathrm{d}r$.

3. Results and discussion

3.1. Microstructure of an "early age" lime–cement–sand mortar

Lime–cement–sand mortar up to the age of 7 day-old has been designated as "early age."

Regardless of the type of lime replacing cement, microscopy shows that, after seven days of hydration, in the case of small percentages of substituted lime, mortars exhibit the same texture as that of a cement–sand reference mortar. In other words, in practically all cases, clusters of $Ca(OH)_2$ platelets were observed in the matrix along with small C–S–H fibres, which cover the anhydrous grains of calcium silicate and which according to Feldman and Sereda [21] give the grains their "porcupine"-like appearance (Fig. 1). In a study of the mechanical strength of the hardened material, it has been noted that the substitution of cement by a small percentage of lime (less than 6%) in an "early-age" lime cement mortar did not influence strengths [15].

Early age mortars with a higher substitution percentage show modifications in the cement paste: C–S–H appears to develop with greater ease than the Portlandite (Fig. 2).

Moreover, when magnesium hydroxide replaces the cement, a new species develops within the matrix. XRD analysis shows that this new species is composed essentially of magnesium and contains very little calcium (Fig. 3 and Table 4). In 7 day-old mortars, this new species appears primarily on the sides of cracks present in the matrix (Fig. 4).

In the case of 28 day-old mortars, however, it can be observed that this new species appears in all of the matrices without causing cracks in the matrix (Fig. 5). In the case of older mortars, it should also be pointed out that the development of this species does not depend on the percentage of $Mg(OH)_2$ being substituted for cement.

Furthermore, the crystallisation of this new species would seem to be the cause of the differences obtained in overvalued Young's modulus values due to the type of lime being substituted. The overvalued Young's modulus values, which have

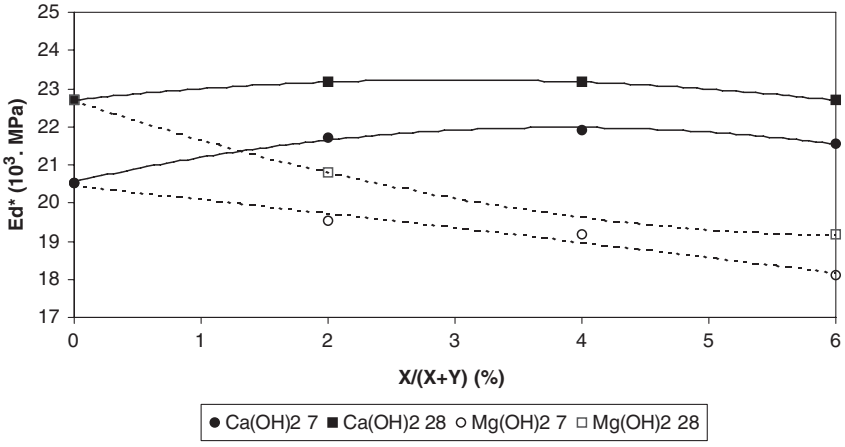

Fig. 6. Variation of the overvalued Young's modulus as a function of mortar age and of type and percentage of substitution lime (constant W/B ratio).

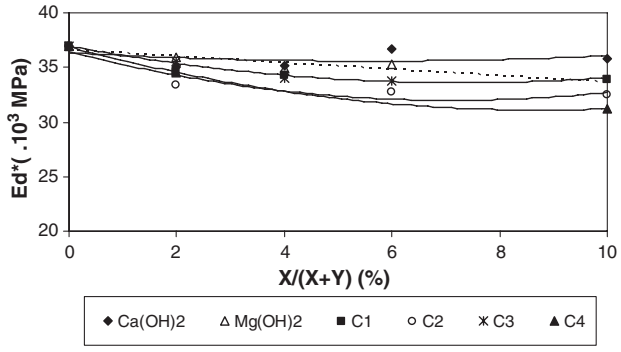

Fig. 8. Evolution in mortar overvalued dynamic elasticity modulus for 2 year-old mortars as a function of both the type and percentage of lime being substituted for cement (constant water content).

been derived in the case of cement substituted by magnesium hydroxide, are smaller than those measured in the case of substitution by calcium hydroxide (Fig. 6).

The study of the mechanical strength of 28-day old mortars as a function of the type of substituted lime leads to the same finding [15]. The evolution in mechanical strength as a function of the percentage of substituted lime varies according to the nature of the substituted lime. In the case of $Ca(OH)_2$ and C_1, mechanical strength increases slightly over the range of 0–4% substituted lime and then decreases as the lime percentage increases. In the case of $Mg(OH)_2$ and lime C_3, however, the evolution in mechanical strength is completely opposite: strength values decrease as lime proportion increases.

Moreover it should be noted that the new species is stable, given the fact that it does not disappear during mortar hydration. But identification of this species is difficult, probably because of the small proportion of this species within the matrix and its degree of crystallinity.

3.2. Appearance of 2 year-old mortars

3.2.1. Appearance of the matrix

Microscopy of two year old mortars produced with constant W/B shows that the replacement of cement by a small percentage of lime rarely modifies the mortar microstructure, except in the case of by lime C_2 utilization. In this particular case, the onset of microporosity in the cement paste, due to the differential crystallisation of hydrates, is definitely noticeable. These hydrates thereby appear as a mix of large platelets and non-contiguous small clusters (Fig. 7).

In contrast, if the percentage of substituted lime increases and equals or exceeds 10%, microcracks appear for the majority of limes tested; these cracks in turn make the matrix less compact. This decrease in matrix compactness would seem to explain the slight decrease in the overvalued dynamic elastic modulus observed as a function of the percentage of cement-substituted lime (Fig. 8).

Only the substitution using lime C_2 actually yields a mortar displaying an altered structure; its matrix is practically the same as that observed with a smaller percentage of substituted lime (i.e. a mix of large platelets and small clusters). In this case, however, the clusters are tightened, a condition that induces lower porosity in the matrix microstructure.

Observation results are summarized in Table 5.

When mortars are made by holding workability constant, it is apparent that the matrices of the various mortars are less compact than that of a "normal" mortar, even when the percentage of lime being substituted is higher. That seems to be normal considering that there is of course a higher water demand. In this case, the decrease in compactness, coupled with an increase in porosity, serves to explain the decrease in elastic modulus obtained as a function of the lime substitution percentage.

3.2.2. Species appearing in mortar "air voids"

At age of 120 days, it can be noticed that the nature of species developing within "air voids" of mortars prepared with a constant W/B ratio varies depending on the type of lime being substituted. In the case of a cement–sand reference mortar, microscopy reveals that hydrated calcium mono-sulfo-aluminate is formed in an air void, appearing in the form of hexagonal platelets with sides measuring between 2 and 5 μm (Fig. 9a). After 2 years, this mono-sulfo-aluminate almost completely covers the surface of the air void trace (Fig 9b).

Table 5
Summary of observation results according to the nature of the substituted lime when the ratio W/B is maintained constant

Microstructure of the matrix for different ages of the mortar			Development of hydrated calcium mono-sulfo-aluminate in mortar air voids
Lime	Early age	2 years old	
$Ca(OH)_2$	Only for high percentages: development of C–S–H with greater ease than $Ca(OH)_2$	Different crystallisation of hydrates: mix of large platelets and clusters ⇒ onset of microporosity. For high substituted percentage: altered structure (microcracks in the matrix)	The observed hydrate crystals are always hexagonal but smaller than those of a cement–sand reference mortar
C_1			
C_2			
C_3		Development of the new species essentially composed of magnesium in all of the matrices without causing cracks in the matrix. This new species is stable.	Infrequent tablets with poorly defined shape
C_4			
$Mg(OH)_2$	Development of a new species essentially composed of magnesium primarily on the sides of cracks		Development entirely stopped

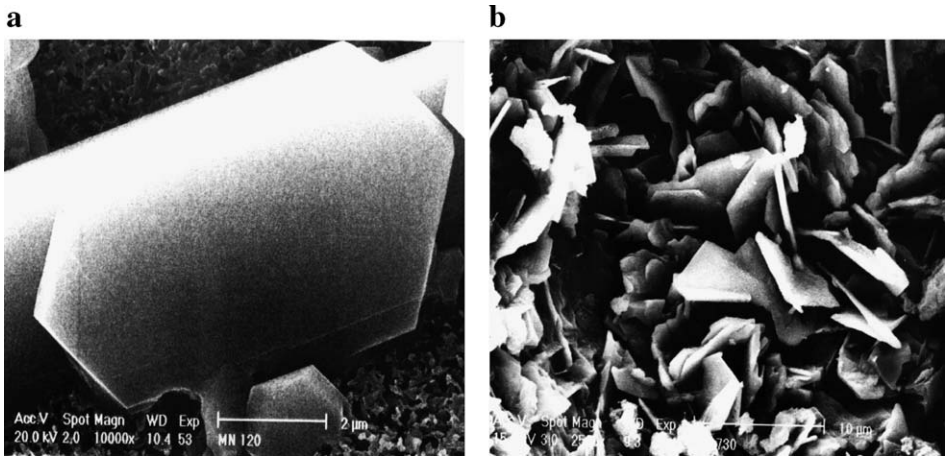

Fig. 9. Scanning electron micrographs of the trace of an air void in a cement–sand reference mortar (constant W/B ratio), a: 120 day-old mortar, the trace on the micrograph corresponds to 2 µm; b: 2 year-old mortar, the trace on the micrograph corresponds to 10 µm.

When a portion of the cement is replaced by calcium hydroxide, smaller hexagonal hydrate crystals of hydrated calcium mono-sulfo-aluminate are observed, regardless of the percentage of substituted $Ca(OH)_2$ (Fig. 10). These results are in agreement with the research conducted by Collepardi et al. [22], who attribute this difference in crystallisation to a slower C_3A hydration speed by virtue of adding $Ca(OH)_2$ to the mortar composition.

Moreover, replacing the cement by magnesium hydroxide seems to almost entirely stop the development of the calcium mono-sulfo-aluminate in empty spaces of the matrix.

In the case of lime C_3, composed using both calcium and magnesium hydroxides, several tablets of calcium mono-sulfo-aluminate can be observed, albeit infrequently and with a poorly defined shape (Fig. 11a). Long fibres of ettringite, measuring up to 10 µm, have also been observed (Fig. 11b).

The same observations have been made in the case of substitution using lime C_4, once again with mixes including both $Ca(OH)_2$ and $Mg(OH)_2$.

Observation results according to the nature of the substituted lime are summarized in Table 5.

It should be noted that if during the substitution of cement by lime the water content of the mortar was allowed to vary (in order to work at a regular consistency), the appearance of new species would be incited within matrix air voids. When the lime being substituted into the cement is either pure calcium hydroxide or lime C_1, poorly crystallised clusters of fibre tufts are particularly noticeable and become even more numerous as the lime substitution percentage increases.

When the cement is replaced by magnesium hydroxide, this species is not present in the empty spaces even if the quantity of water varies. In this substitution case, the production of mortars at constant workability does not seem to influence the development of species in the mortar's empty spaces.

4. Conclusion

The aim of the present work has been to determine the effect of replacing a percentage of cement by lime on the evolution of mortar microstructure. Various categories and proportions of lime have been tested by holding the total binder/sand ratio constant.

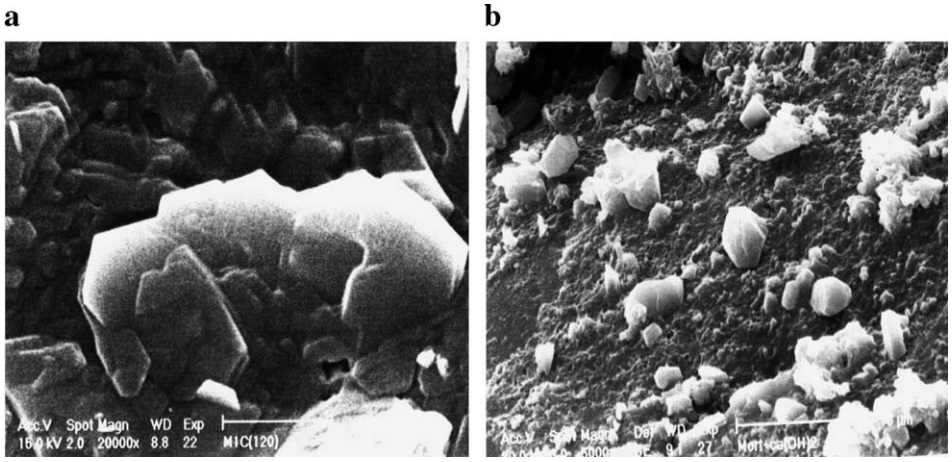

Fig. 10. Scanning electron micrographs of the trace of an air void (constant W/B ratio), a: in a mortar in which 4% of the cement has been replaced by $Ca(OH)_2$, the trace corresponds to 1 µm; b: in a mortar in which 10% of the cement has been replaced by $Ca(OH)_2$, the trace corresponds to 5 µm.

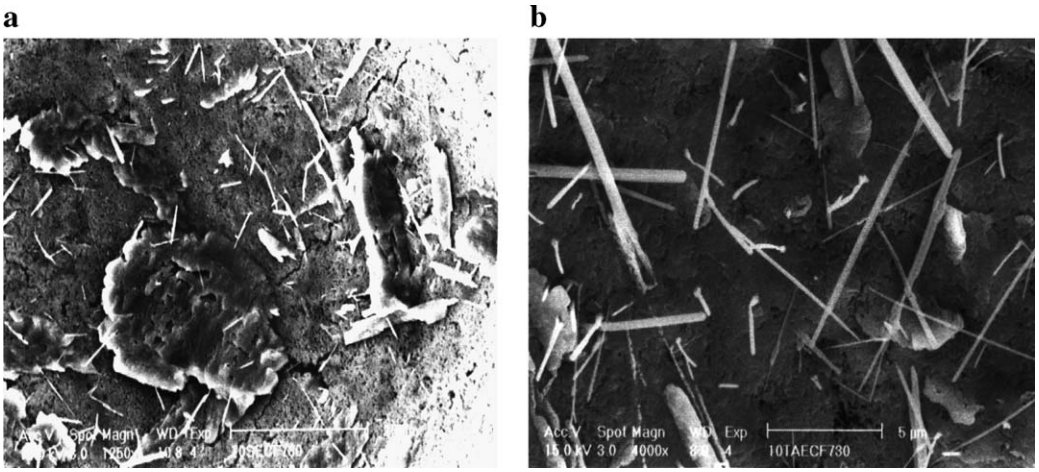

Fig. 11. Scanning electron micrographs of the trace of an air void in a 730 day-old mortar in which 10% of the cement has been replaced by lime C_3, a: the trace on the micrograph corresponds to 20 μm, b: the trace on the micrograph corresponds to 5 μm.

At the same time, experimental results have allowed highlighting the influence of chemical nature, morphology, lime content and water/binder ratio. For the majority of limes used herein, the substitution of a small percentage of cement by lime does not modify the microstructure of the mortar matrix, except in the case of a magnesian lime or a calcic lime featuring sizeable specific surface area. This finding is due to the fact that under both of these conditions, the crystallisation of hydrates differs entirely.

In contrast, for a higher lime substitution percentage, the replacement of cement with fine lime particles induces modification of the mortar microstructure, which is revealed either by the presence of microcracks in the matrix or by an alternative hydrate development in the case of calcium hydroxide with a significant specific surface area.

The visualisation of "air voids", which exist in the mortar and constitute empty spaces, has also highlighted the prominent role played by the composition and nature of the substituting lime in developing the component species of the matrix.

Although the obtained results require still in-depth analysis, they are important. Indeed the study of the microstructure enabled to raise the problem of the choice of the kind of lime in the lime–cement mortars.

References

[1] V.S. Ramachandran, Proceedings of the 8th International Congress on the Chemistry of Cements, Rio de Janeiro, 22–27 September, 1986, Finep, Rio de Janeiro, 1986, p. 109.
[2] C. Neto, V. Campiteli, The influence of limestone additions on the rheological properties and water retention value of Portland cement slurries in carbonate additions to cement, in: Klieger/Hooton (Ed.), ASTM STP 1064, USA, 1990, p. 24.
[3] A. Kronlof, Effect of very fine aggregates on concrete strength, Materials and Structures 27 (1994) 15–25.
[4] J.L. Gallias, U.H. Gaboriau, P. Le Berre, Proceedings of the Conchem — International Exhibition and Conference, Scotland, 1995, E and Fn Spon, Scotland, 1995, p. 161.
[5] J.L. Gallias, S. Aggoun, R. Cabrillac, R. Kara-Ali, Proceedings of the International RILEM Conference on Production Methods and Workability of Concrete, Scotland, 1996, E and Fn Spon, 1996, p. 523.
[6] H. Uchikawa, S. Hanehara, H. Hirao, Influence of microstructure o the physical properties of concrete prepared by substituting mineral powder for part of fine aggregate, Cem. Concr .Res. 26 (1996) 101–111.
[7] R.F. Runova, M.A. Kochevykh, I.I. Rudendo, Pressed ash containing concrete: activation of structure formation, in: E and Fn Spon (Ed.), Concrete for Environment and Protection, Scotland, 1996, pp. 671–676.
[8] F. De Larrard, Ultrafine particles for the making of very high strength concrete, Cem. Concr. Compos. 21 (1999) 172–189.
[9] J. Pera, S. Husson, B. Guilhot, Influence of finely ground limestone on cement hydration, Cem. Concr. Compos. 21 (1999) 99–105.
[10] W. Sriboonlue, E.M. Wallo, The effect of constituent proportions on stress–strain characteristics of Portland cement–lime mortar and grout, in: J.H. Matthys (Ed.), Masonry: Components to Assemblages, ASTM STP, vol. 1063, 1990, Philadelphia.
[11] P.C. Philippi, P. Rosendo Yunes, C.P. Fernandes, F.S. Magnani, The microstructure of porous building materials: study of a cement and lime mortar, Transp. Porous Media 14 (1994) 219–245.
[12] P.C. Philippi, H.A. Souza, Modelling moisture distribution and isothermal transfer in a heterogeneous porous material, Int. J. Multiph. Flow 21 (4) (1995) 667–691.
[13] A. Colantuono, S. Dal Vecchio, O. Marino, G. Mascolo, A. Vitale, Cement–lime mortars joining porous stones of masonries able to stop the capillary rise of water, Cem. Concr. Res. 26 (6) (1996) 861–868.
[14] Y. Sébaïbi, R.M. Dheilly, M. Quéneudec, Study of the water-retention capacity of a lime–sand mortar: influence of the physicochemical characteristics of the lime, Cem. Concr. Res. 33 (2003) 689–696.
[15] Y. Sébaïbi, Influence d'une chaux magnésienne de type «S» sur les propriétés d'un mortier de ciment Portland, comparaison avec d'autres chaux, Thesis, INSA de Lyon, Lyon, 2000.
[16] R.S. Boynton, in: John Wiley and Sons (Ed.), Chemistry and Technology of Lime and Limestone, 1966, New York.
[17] A.M. Neville, Properties of Concrete, Longman Editions, England, 1995.
[18] R. Jones, Les essais non destructifs des bétons, Eyrolles Editions, Paris, 1967.
[19] S. Brunauer, P.H. Emmet, E. Teller, Adsorption of gases in multimolecular layer, J. Am. Chem. Soc. 60 (1938) 309.
[20] E.P. Barret, L.G. Joyner, P.P. Halenda, The determination of the pore volume and area distributions in porous substances: I Computations from nitrogen isotherms, J. Am. Chem. Soc. 73 (1951) 373.
[21] R.F. Feldman, P.J. Sereda, A model for hydrated Portland cement paste as deduced from sorption-length change and mechanical properties, Mat. Struct. 1 (6) (1968) 509–520.
[22] H. Collepardi, M. Corradi, G. Baldini, M. Pauri, Meccanismo d'aziane del gess sur idrazione dell' aluminato tricalcico, Il cemento, 1978, pp. 169–176.